Determination of transition energies and oscillator strengths in GaAs-$Al_xGa_{1-x}As$ multiple quantum wells using photovoltage-induced photocurrent spectroscopy

P. W. Yu
University Research Center, Wright State University, Dayton, Ohio 45435

G. D. Sanders
Universal Energy Systems, Inc., 4401 Dayton-Xenia Road, Dayton, Ohio 45432

D. C. Reynolds, K. K. Bajaj, and C. W. Litton
Electronic Research Branch, Avionics Laboratory (AFWAL/AADR), Air Force Wright Aeronautical Laboratories, Wright-Patterson Air Force Base, Ohio 45433

J. Klem, D. Huang, and H. Morkoç
Department of Electrical and Computer Engineering, University of Illinois at Urbana-Champaign, 1406 West Green Street, Urbana, Illinois 61801-2991
and Coordinated Science Laboratory, University of Illinois at Urbana-Champaign, 1101 West Springfield Avenue, Urbana, Illinois 61801-3082

(Received 6 February 1986; revised manuscript received 20 October 1986)

A careful study of excitonic lines in the photocurrent spectra of GaAs-$Al_{0.25}Ga_{0.75}As$ multiple-quantum-well structures grown by molecular-beam epitaxy is carried out for wells having widths in the range 35—245 Å. Transition energies and relative oscillator strengths are measured and compared with theoretical values obtained using a multiband effective-mass approach, and excellent agreement between experimental data and theory is found. A large number of transitions, as many as 13 excitons of both allowed and forbidden types, are identified and their anomalously large oscillator strengths are shown to be the result of strong mixing of valence subbands.

I. INTRODUCTION

Several studies of quantum size effects in GaAs-$Al_xGa_{1-x}As$ quantum-well structures have been made using purely optical techniques such as photoluminescence (PL),[1,2] absorption,[3] and reflection.[4,5] Recently, photocurrent (PC) techniques[6–10] employing optical and transport methods simultaneously have also been used for the characterization of quantum wells. These studies suggest that PC techniques can provide information equivalent to that obtained using the above-mentioned purely optical measurements. The PC spectra in quantum wells are shown to be proportional to absorption spectra[11] for the intrinsic optical transitions. Moreover, PC measurements do not require the substrate etching processes required for absorption measurements which may cause strain in quantum wells. However, PC measurements do involve application of an electric field which changes the intrinsic transition energy[6,8,11,12] (Stark shift), the transition strength,[12] and the transition lifetime.[13]

In this paper we investigate the photovoltage-induced photocurrent response of GaAs-$Al_{0.25}Ga_{0.75}As$ multiple-quantum-well (MQW) structures grown by molecular-beam epitaxy (MBE). The well width of the structure studied ranges from 35 to 245 Å. A large number of transitions, as many as 13 excitons of both allowed ($\Delta n=0$) and forbidden ($\Delta n\neq 0$) types, were observed. The transition energies were used to assess the conduction- and valence-band discontinuities. The PC response which is proportional to the exciton transition strength allowed us to measure the relative exciton oscillator strengths for a large number of transitions as a function of well width for the first time to the best of our knowledge. The measured transition energies and oscillator strengths were then compared with calculated values obtained from a theory incorporating the valence subband mixing effects. Also, the effects on the transition energies and oscillator strengths due to a slight quantum-well asymmetry were investigated. The measured and calculated values were in good agreement. In particular, such a systematic study involving the forbidden excitons is necessary in order to provide a stringent quantitative test of the predictions of the valence-band mixing models since the strength of forbidden excitons arises entirely from the mixing effects. To our knowledge this work represents the first such study and as such represents the best experimental confirmation of the valence subband mixing theories. In addition, the sharing of oscillator strength between the $C2$-$H3$ and $C2$-$L2$ excitons is also observed for the first time. (The notation Cn-Hm and Cn-Lm will be explained in Sec. III.)

II. EXPERIMENTAL DETAILS

The samples used in the experiment were grown by MBE on Si-doped n^+-type GaAs substrates. The samples consist of an n^+-type substrate followed by a 0.5—1.0-μm buffer layer and 0.8—1.2-μm MQW structure. The

widths of the $Al_{0.25}Ga_{0.75}As$ barrier L_B were 100 Å for all the samples measured and the well width L_z ranged from 35 to 245 Å. The buffer layer and MQW structure were nominally undoped. Details for crystal growth have been described elsewhere.[14]

A Schottky-barrier configuration prepared by evaporating a semitransparent Au film on the GaAs layer of the MQW structure was used for PC measurements. Thus, a built-in electric field perpendicular to the interfaces was set up between the Schottky barrier and an In Ohmic contact on the n^+-type GaAs substrate. The Au film consisted of a rectangular area (1×2 mm^2) of $\sim$200-Å thickness. The flat-band condition was estimated to occur close to an external voltage of 0.4—0.8 V for the investigated samples. These estimates are based on (i) an open-circuit photovoltage measurement with a Kr^+-ion laser operating above the $Al_{0.25}Ga_{0.75}$-As band gap and (ii) a PL intensity variation measurement depending on an external dc voltage. A photovoltage is measured when it saturates for high excitation intensities. This value was assumed to be equal to the built-in voltage. PL intensity and peak energy were measured on the electrode, off the electrode and with an external voltage. A comparison of PL intensities under these three situations provided an estimate of the flat-band condition. The PC spectrum was obtained by measuring the PC as a function of the wavelength of the incident light focused on the Schottky electrode. The variable wavelength light source was a tungsten-iodine lamp dispersed through an $f=1$-m grating monochromator. The wavelength resolution of the light typically was $\sim$3 Å. A lock-in amplifier was used for standard synchronous detection. The sample was mounted in a Janis variable temperature dewar. PL measurements were made using the 6471-Å line of a Kr^+ ion laser with an excitation intensity of 10^{-3}—10 W/cm^2. The PL signal was dispersed by an $f=1.26$-m Spex spectrometer and was detected with a cooled GaAs cathode photomultiplier tube.

III. ANALYSIS

When one considers the photovoltage-induced photocurrent from an MQW structure shown schematically in Fig. 1 over the energy range between the GaAs and $Al_{0.25}Ga_{0.75}As$ band gaps the primary PC components originate from regions (a) and (b). The regions (a) and (b) include, respectively, the Schottky-barrier interface—MQW structure and the GaAs buffer—n^+-type GaAs substrate. Owing to the Schottky barrier a built-in electric field perpendicular to the quantum wells can be present in the MQW as well as the GaAs buffer layer. The PC component from region (a) and region (b) arises, respectively, from carriers tunneling through barrier regions in the MQW and from carriers in the buffer layer. When tunneling becomes dominant one finds that the exciton absorption peaks coincide with the relative maxima (peaks) of the PC response. When the carriers generated by optical absorption in the MQW remain trapped in the well, the carriers from the buffer—n^+-type-GaAs region become dominant and the PC response due to an excitonic transition will appear as a relative minimum (dip) in the

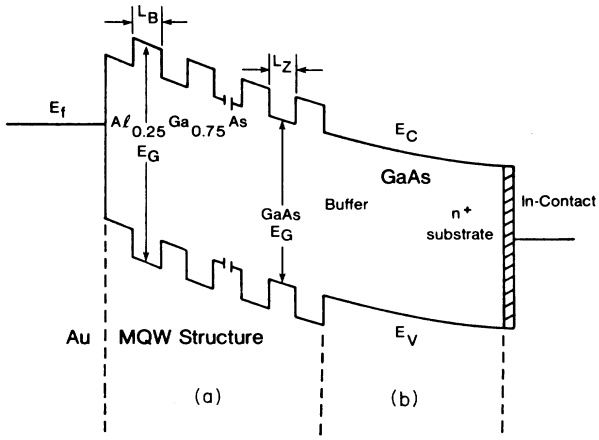

FIG. 1. Schematic structure of samples used for photocurrent measurements.

PC response at the corresponding exciton absorption. This is because the intensity of light falling on region (b) is modified by the absorption of the MQW structure. When one of the two PC mechanisms is dominant, the energies and strengths of the minima (maxima) can be taken to be the exciton transition energies and the exciton oscillator strengths in arbitrary units, respectively. However, these values are correct when the electric field in the MQW structure does not modify the exciton transition energy and oscillator strength. In the present experiment, the minima and the integrated areas of the minima were used to obtain the exciton transition energy and oscillator strength, respectively.

For the analysis of our results in terms of transition energy, transition strength and transition line shape a multiband effective-mass approach[14] including valence-band mixing effects was used. Exciton transitions are labeled with the notation *Cn-Hm* and *Cn-Lm* throughout this paper, where *Cn-Hm* represents an exciton associated with the nth electron and mth heavy-hole subband at $\mathbf{k}=\mathbf{0}$ and *Cn-Lm* denotes an exciton related to the mth light-hole subband. The energy levels and envelope functions are obtained variationally and the subband variational energies are corrected by adding a constant correction factor obtained by exactly solving the Hamiltonian[14] at $\mathbf{k}=\mathbf{0}$, where a simple particle-in-a-box description[15] applies for both electrons and holes. The correction factor is the difference between the exact and variational energies at $\mathbf{k}=\mathbf{0}$. The band-gap discontinuity between the GaAs and $Al_xGa_{1-x}As$ is taken to be $\Delta E_g(x)=1.115x+0.37x^2$ eV.[16] The depths of the confining potentials for electron and hole, V_e and V_h are defined as $V_e=Q_e\,\Delta E_g$ and $V_h=Q_h\,\Delta E_g$, where Q_e and Q_h are the band offset parameters. The calculated exciton transition energy E_{nm} is given by

$$E_{nm}=E_g^{\mathrm{GaAs}}+E_n^e+E_m^h-E_{nm}^B\ , \tag{1}$$

where E_g^{GaAs} is the band-gap energy of GaAs, E_n^e and E_n^h are the nth electron and mth hole subband energies at

$\mathbf{k}=0$ and E_{nm}^{B} is the exciton binding energy for the transition $Cn\text{-}H(L)m$. E_{nm}^{B} is calculated[14] using the multiband effective-mass approach. The model incorporates the effects of valence-band mixing and nonparabolic valence subbands. Inclusion of valence-band mixing yields somewhat larger exciton-binding energies for excitons whose valence subbands have negative zone center effective masses. Also, the valence-band mixing leads to a sharing of oscillator strength between the allowed and forbidden transitions. To approximate the experimental situation, the computed band-to-band and exciton absorption are assumed to be broadened by Lorentzian functions of half-widths Γ_b and Γ_x, respectively, for each transition. Values of Γ_x and Γ_b are given by

$$\Gamma_{b,x}=C_0 n_e n_h \ , \tag{2}$$

where n_e and n_h are principal quantum numbers for electrons and holes, and C_0 is an adjustable constant determined by the experimental linewidths.

The absorption coefficient for the $Cn\text{-}H(L)m$ exciton, α_{nm}, is related[17] to the oscillator strength per unit area f_{nm} for light propagating along the crystal growth direction by

$$\alpha_{nm}=\frac{4\pi^2 e^2 \hbar f_{nm}}{n_0 m_0 C L_z}\Delta(\hbar\omega-E_{nm}) \ , \tag{3}$$

where $\Delta(\hbar\omega-E_{nm})$ is a Lorentzian line-shape function, n_0 is the refractive index, and m_0 is the free-electron mass. The oscillator strength f_{nm} is calculated by the multiband effective-mass model described in Ref. 14. The integrated absorption peak area due to the $Cn\text{-}H(L)m$ exciton, A_{nm} (in units of eV cm^{-1}), is proportional to f_{nm} and is given by

$$A_{nm}=\frac{4\pi^2 \hbar e^2 f_{nm}}{L_z m_0 n_0 C} \ . \tag{4}$$

However, the PC response is measured in arbitrary units in our experiment. Thus, experimental oscillator strength can only be described relative to a given exciton transition.

The transition energy E_{nm} and the absorption coefficient α_{nm} of the $Cn\text{-}H(L)m$ exciton were primarily calculated for a symmetrical square well. The calculation was extended in order to study possible effects arising from a slight asymmetry of the square well. The band-gap discontinuity between the GaAs and $Al_xGa_{1-x}As$, $\Delta E_g(x)$, is uniform over the well width L_z for a symmetric square well. To study effects of possible asymmetry of the well a linear variation of $\Delta E_g(x)$ over L_z was assumed due to variation of x in the well: $\Delta E_g(x)$ is assumed to decrease linearly from $\Delta E_g(x)$ to $A(x')=\Delta E_g(x)-\alpha(x')$, where $\alpha(x')$ is the energy difference between the $Al_{x'}Ga_{1-x'}As$ and GaAs band gaps and x' is the aluminum concentration inside the well of L_z.

IV. RESULTS AND DISCUSSION

The MQW structures in the present experiment experience a built-in electric field perpendicular to the wells as shown in Fig. 1. Thus, the exciton transition energy and oscillator strength were examined as a function of external voltage to study a possible modification of these values. All the PC measurements were made under conditions where the PC responses appear as relative minima. This was done in order to minimize possible errors in determining the oscillator strength caused by carrier tunneling from the MQW structure.

Figure 2 shows a $T=77$-K PC spectrum with external voltages V of 0 ($\sim 3\times 10^3$ V/cm), $+0.5$, and -1.5 V for a well of $L_z=245$ Å. The bias of $+0.5$ V approximately corresponds to the flat-band condition. No discernible change in the exciton transition energies and oscillator strengths were observed for the spectra obtained with 0 and $+0.5$ V. The dips in the PC spectra are interpreted as exciton absorption transitions whereas the background PC responses are attributed to the band-to-band absorption. The identified excitons are labeled for 13 transitions. However, we note that the increase of a reverse-bias of -1.5 V enhances the transition strength of the $C2\text{-}H1$ exciton and a new transition on the higher-energy side of the $C2\text{-}H4$ exciton (the new transition has yet to be identified). This is shown in Fig. 2(c) for the PC spectrum obtained with $V=-1.5$ V. The transition strength of other excitons also increases relative to that of the $C1\text{-}H1$ exciton. However, the details of change due to the applied electric field is not the subject of the present work and will be discussed in a future publication. Thus, our

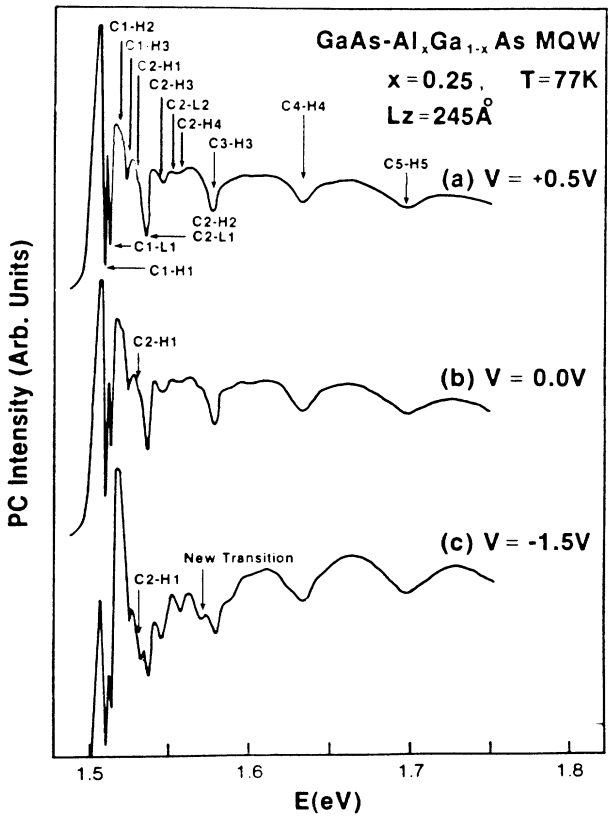

FIG. 2. Photocurrent spectra of a 245-Å well obtained with external voltages of $V=0.5$, 0, and -1.5 V.

present discussion is limited to demonstrating the fact that the exciton transition energy and oscillator strength do not show any discernible changes for external voltages in the range $V=0$–0.5 V for the well of width $L_z=245$ Å. Simple perturbation theory calculations show that the shifts in the subband energies are proportional to E^2 (E is an electric field). The fact that no appreciable shift in subband energies is observed when the applied field is varied about the measured flat-band voltage is a further strong indication that the built-in voltage has in fact been balanced out. This was observed to be true for other samples having narrower well widths than $L_z=245$ Å since a given electric field strength has a smaller perturbing effect on narrower wells.

Figure 3 shows the optical spectra obtained with PL and PC for the sample with $L_z=245$ Å in the temperature range 2–296 K. The PC and PL measurements were made, respectively, under $V=0$ V and the off-electrode condition. The observed exciton transitions were identified for both PL and PC spectra as shown in the figure. The identified exciton transition energy at different temperature shows that (i) the transition energies obtained using PL and PC coincide well and thus the exciton transition energy obtained by PC does not show any discernible change with an external bias of 0 to $+0.5$ V (the flat-band condition), and (ii) the excitonic transitions shift with temperature such that all the transitions remain at fixed energies relative to the known temperature variation of the GaAs band gap.

Energies of the observed transitions relative to the $C1$-$H1$ transition energy are plotted as a function of well width in Fig. 4 for the $C1$-$L1$, $C1$-$H3$, and $C3$-$H3$ transitions in order to compare with theoretical exciton transition energies assuming various hole masses. The theoretical results are based on the multiband effective-mass model[14] which gives the variation in the exciton binding energy for different transitions. The hole masses considered are (a) $m_h^*/m_0=0.34$ and $m_l^*/m_0=0.094$ (Ref. 18), (b) $m_h^*/m_0=0.38$ and $m_l^*/m_0=0.09$ (Ref. 19), and (c) $m_h^*/m_0=0.45$ and $m_l^*/m_0=0.087$ (Ref. 20). All the calculations are made with the band offset parameter $Q_e=0.6$. As shown in Fig. 4, the experimental data are in good agreement with theory when the masses of case (a) are used.

The experimental transition energies relative to the $C1$-$H1$ transition energy are also plotted as a function of well width in Fig. 5 in order to study any effect due to the asymmetry of the well. The wells considered are (i) a symmetrical square well with $\Delta E_g(x=0.25)$, (ii) an asymmetrical well with $\Delta E_g(x=0.25)$ and $A(x'=0.05)$, and (iii) an asymmetrical well with $\Delta E_g(x=0.25)$ and $A(x'=0.1)$. The parameters used are $m_h^*/m_0=0.34$, $m_l^*/m_0=0.094$, and $Q_e=0.6$. The comparison with experiment clearly indicates that the MQW structures used in the present experiment are symmetric. A slightly asymmetric well results in higher transition energies compared to square wells due to the increased effective gap.

Energies of all the observed transitions relative to the $C1$-$H1$ transition energy are plotted as a function of well width in Fig. 6 for all the samples measured. Also included in Fig. 6 are theoretical results calculated with $m_h^*/m_0=0.34$, $m_l^*/m_0=0.094$, and $Q_e=0.6$. The agreement between the calculated and experimental transition energies are in general quite good except for the $C1$-$H2$ transitions for well width $L_z>200$ Å. We believe the discrepancy of ~ 1 meV may be attributed to the failure of the present exciton model to take into account correlation of electron and hole motion along the crystal growth direction (adiabatic approximation). For narrow

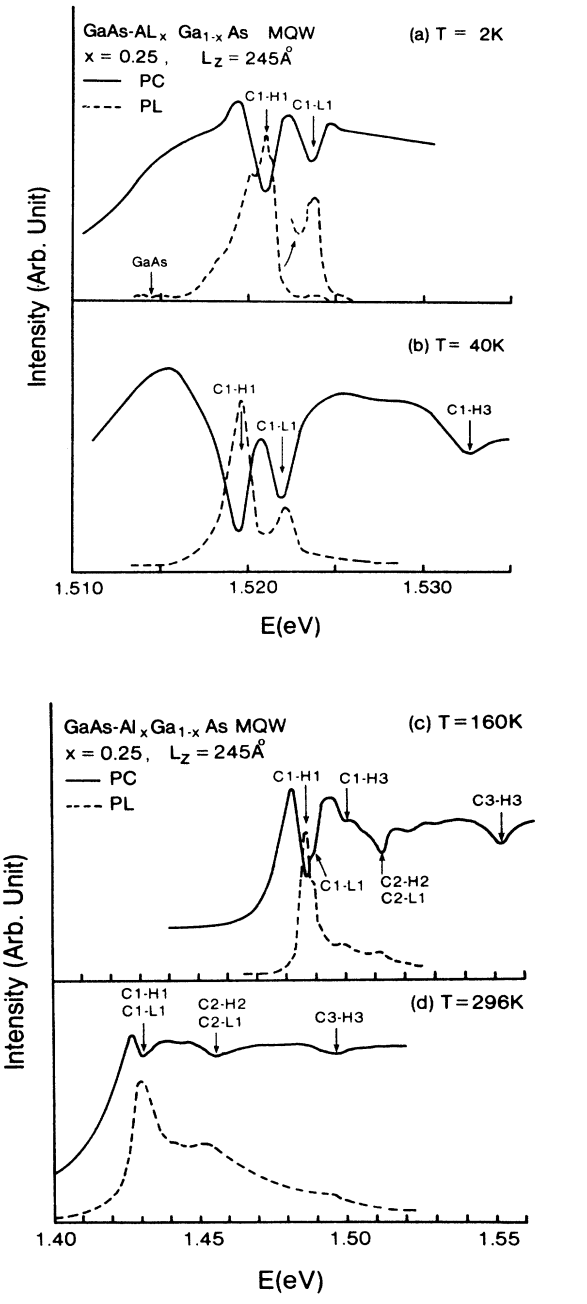

FIG. 3. Comparison of exciton transition energies of a 245-Å well obtained using photoluminescence and photocurrent methods at temperatures 2, 40, 160, and 296 K.

wells this adiabatic approximation used in Ref. 14 is quite satisfactory but breaks down for wider wells.[14] However, it is clear that the calculation made with the above parameters of hole masses and band offset parameter yields better results compared to the other hole masses. The electron mass used is $m_e^*/m_0=0.067$. Thus, these values of $m_h^*/m_0=0.34$, $m_l^*/m_0=0.094$, and $Q_e=0.6$ were used for calculations throughout the present work. The choice of these hole masses will also be discussed later in connection with the oscillator strength measurements of excitonic transitions.

Figures 7(a)—7(c) show the measured PC responses and calculated absorption spectra for MQW structures with $L_z=107$, 150, and 245 Å. In generating the calculated exciton spectra, we adjusted c_0 of Eq. (2) to match the data with the values of $c_0=1$—6 meV depending on the transition. The measured and calculated spectra agree well in terms of the exciton transition energy and the oscillator strength. The dominant transitions are due to the allowed ($\Delta n=0$) excitons $C1$-$H1$, $C1$-$L1$, $C2$-$H2$, $C2$-$L2$, $C3$-$H3$, $C4$-$H4$, and $C5$-$H5$. Several forbidden ($\Delta n\neq 0$) exciton transitions are observed, i.e., the $C1$-$H2$, $C1$-$H3$, $C2$-$H3$, $C2$-$H4$, $C3$-$L2$, and $C3$-$H5$. We also note from the experimental and theoretical spectra that the structure due to the $C2$-$L1$ exciton is superposed on the $C2$-$H2$ exciton at the lower-energy side. The observation of the above forbidden transitions is only possible because of the mixing of the heavy- and light-hole states. In particular, the effect of band mixing on the exciton bind-

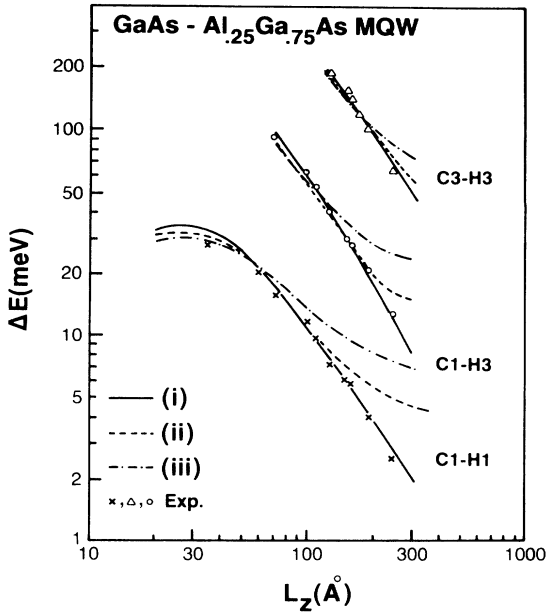

FIG. 5. Measured and calculated transition energies as a function of L_z for GaAs-$Al_{0.25}Ga_{0.75}As$ MQW structures. ΔE is the energy measured from the $C1$-$H1$ exciton transition energy. The calculations are made with $m_h^*/m_0=0.34$ and $m_l^*/m_0=0.094$ for three types of the well: (i) symmetrical wells with $\Delta E_g(x=0.25)$, (ii) asymmetrical wells with $\Delta E_g(x=0.25)$ and $A(x'=0.05)$, and (iii) asymmetrical wells with $\Delta E_g(x=0.25)$ and $A(x'=0.1)$.

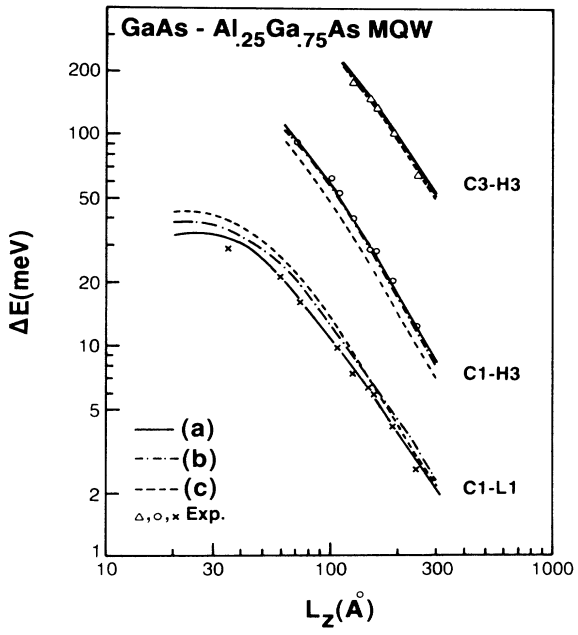

FIG. 4. Measured and calculated transition energies as a function of L_z for GaAs-$Al_{0.25}Ga_{0.75}As$ MQW structures. ΔE is the energy measured from the $C1$-$H1$ exciton transition energy. The calculations are made with three different hole masses: (a) $m_h^*/m_0=0.34$ and $m_l^*/m_0=0.094$, (b) $m_h^*/m_0=0.38$ and $m_l^*/m_0=0.09$, and (c) $m_h^*/m_0=0.45$ and $m_l^*/m_0=0.087$.

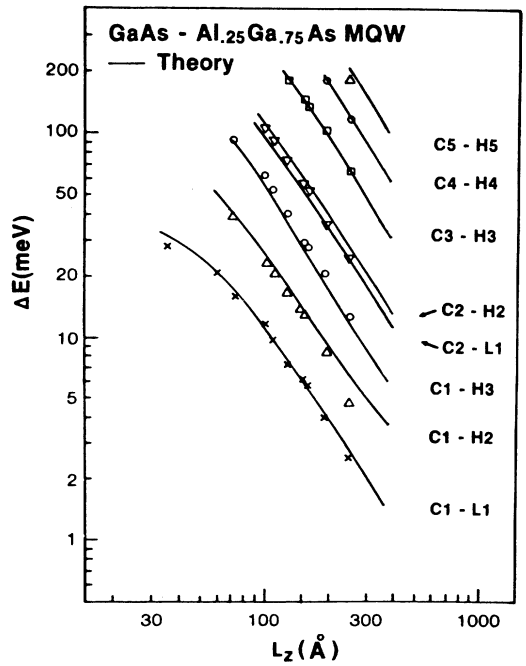

FIG. 6. Measured and calculated exciton transition energies as a function of L_z for GaAs-$Al_{0.25}Ga_{0.75}As$ multiple-quantum-well structures. ΔE is the energy measured from the $C1$-$H1$ exciton transition energy. The solid lines are the theoretical values calculated for symmetrical wells with $\Delta E_g(x=0.25)$.

ing energy is manifested in the enhancement of binding energies for the $C1$-$L1$, $C2$-$L1$, and $C1$-$H3$ excitons relative to other excitons. The enhanced binding energy yields better agreement with experiment (Fig. 6) than results obtained using uncoupled parabolic valence bands. The enhancement of the binding energy arises from the enhancement of the joint density of states due to the valence-band mixing.

A shift in transition strength between a forbidden $\Delta n \neq 0$ transition and an allowed $\Delta n = 0$ transition due to the valence-band mixing were observed for the transitions $C2$-$L1$ and $C2$-$H2$ and the transitions $C2$-$H3$ and $C2$-$L2$. For both cases, the forbidden transitions gain a large transition strength at the expense of the allowed transition. The case for the $C2$-$H2$ and $C2$-$L1$ excitons was discussed[21] recently. Our PC spectra also clearly show the superposition of the two transitions. Similarly, we find a shift of transition strength from the $C2$-$L2$ exciton to the $C2$-$H3$ exciton. The relative strength of these transitions is a sensitive function of the hole masses

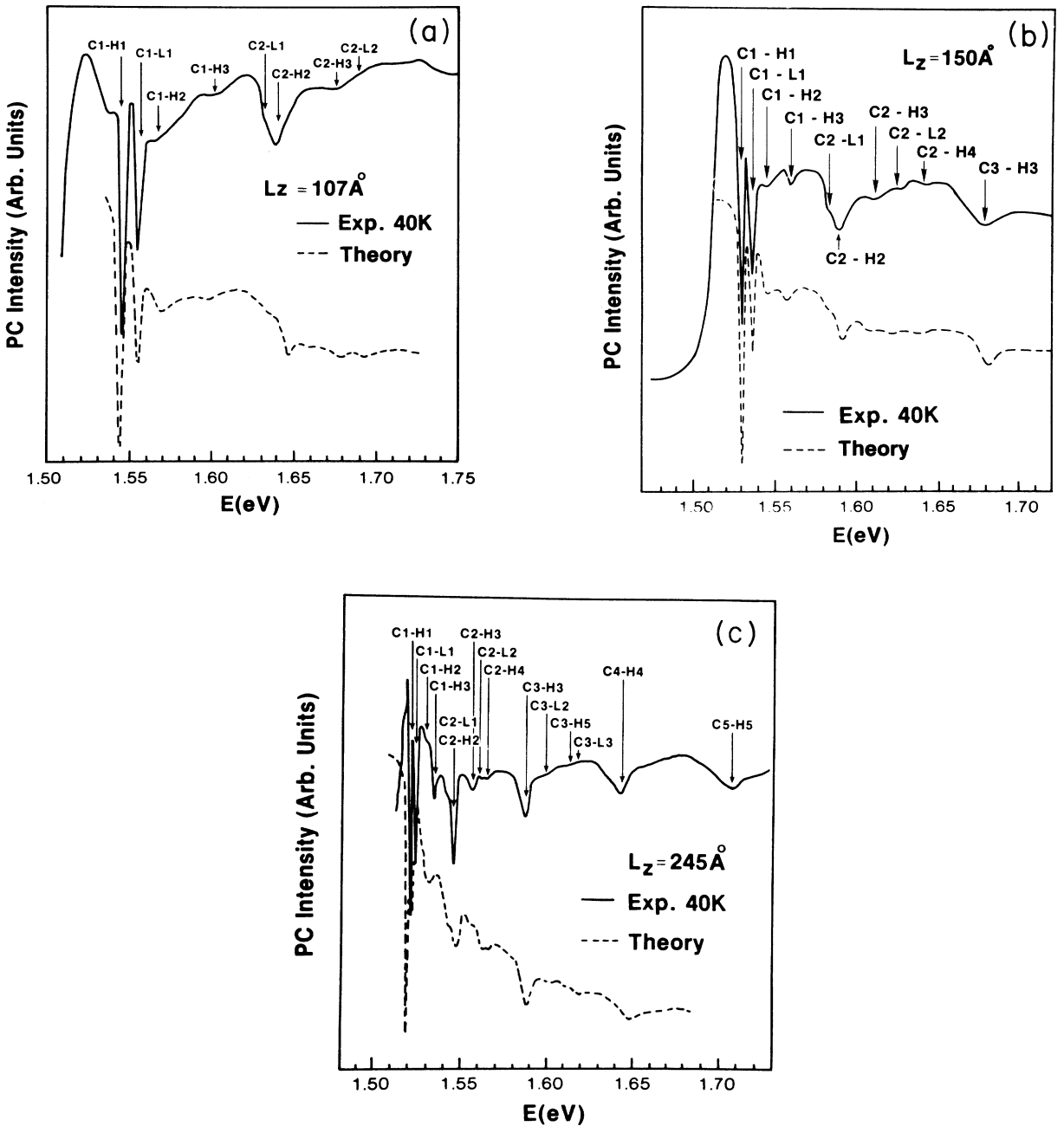

FIG. 7. Measured photocurrent spectra and calculated absorption spectra of multiple-quantum-well samples with (a) $L_z = 107$ Å, (b) $L_z = 150$ Å, and (c) $L_z = 245$ Å. The calculations are made with $m_h^*/m_0 = 0.34$ and $m_l^*/m_0 = 0.94$.

adopted. Figure 8 shows the theoretical absorption spectra of an $L_z = 150$ Å well obtained with three different hole masses: (a) $m_h^*/m_0 = 0/34$ and $m_l^*/m_0 = 0.094$, (b) $m_h^*/m_0 = 0.38$ and $m_l^*/m_0 = 0.09$, and (c) $m_h^*/m_0 = 0.45$ and $m_l^*/m_0 = 0.087$. Distinctive differences among the spectra can be found for the relative strengths of two pairs of transitions; namely, the relative strengths of the forbidden $C2$-$H3$ exciton relative to the allowed $C2$-$L2$ exciton and the forbidden $C2$-$L1$ exciton relative to the allowed $C2$-$H2$ exciton. The oscillator strength of the $C2$-$L1$ and $C2$-$L2$ excitons increased relative to those of the $C2$-$H2$ and $C2$-$H3$ excitons, respectively, with the variation of hole masses from case (a) to case (c). A reversal of the absorption peak position for the $C2$-$L1$ and $C2$-$H2$ excitons is noteworthy. The relative strengths of the forbidden $C2$-$H3$ exciton relative to the allowed $C2$-$L2$ exciton using the hole masses of case (a) are larger by factors of 1.9 and 3.1 compared with results obtained using the hole masses of cases (b) and (c), respectively. The calculated size of the $C2$-$H3$ exciton strength relative to that of the $C2$-$L2$ exciton is consistent with the experimental spectrum as shown in Fig. 7(b) when the masses of case (a) are used. This observation made with the choice of the masses is also consistent with the experimental relative strengths for $C2$-$H2$ and $C2$-$L1$ excitons. The above features from the two pairs of transitions, shown with an $L_z = 150$ Å well, are also true for the wells of $L_z \cong 100$–300 Å. Thus, we think that the masses of case (a) explain well our observed PC spectra. However, we

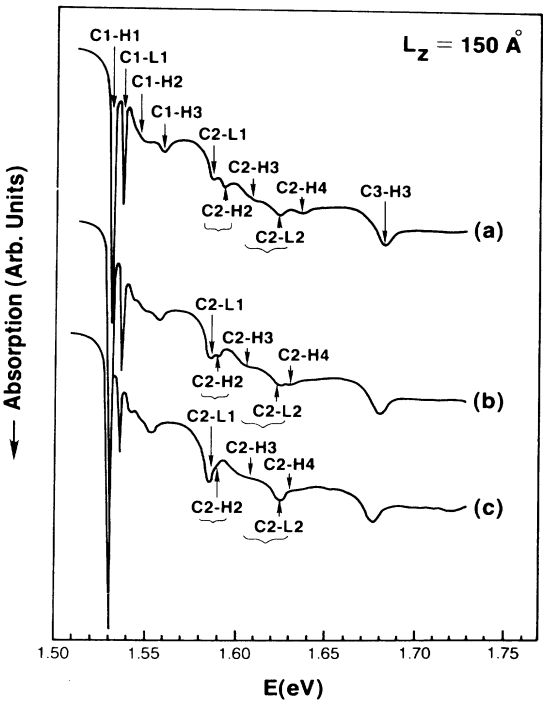

FIG. 8. Calculated absorption spectra for a symmetrical well of $L_z = 150$ Å with three different hole masses: (a) $m_h^*/m_0 = 0.34$ and $m_l^*/m_0 = 0.094$, (b) $m_h^*/m_0 = 0.38$ and $m_l^*/m_0 = 0.09$, and (c) $m_h^*/m_0 = 0.45$ and $m_l^*/m_0 = 0.087$.

also find that the oscillator strengths of other transitions are less sensitive functions of the hole masses compared with the case for the $C2$-$H2$, $C2$-$L1$, $C2$-$H3$, and $C2$-$L2$ excitons.

In order to further verify our identification of the observed excitons, the experimental transition strengths were compared with theoretically calculated oscillator strengths. Experimental values were obtained from the relative integrated area of dips of PC responses, which were measured at 40—80 K. The calculated oscillator strength per unit volume is proportional to f_{nm}/L_z (Ref. 17) where f_{nm} is the oscillator strength per unit area for light propagating along the growth direction. As shown in Eq. (4), f_{nm}/L_z is directly proportional to the integrated area A_{nm} of the absorption peak due to the Cn-$H(L)m$ exciton. Since the PC response was obtained in arbitrary units, the values of experimental oscillator strength were measured relative to the $C1$-$H1$ exciton oscillator strength. Then, the experimental values of the $C1$-$H1$ exciton oscillator strength were adjusted to agree with the theoretical values. Excellent agreement between experimental and theoretical oscillator strengths for the $C1$-$H1$ exciton has been previously established[3] using direct absorption measurements.

It is well known that any asymmetry in the quantum-well structure will result in significant changes in the strength of the forbidden exciton lines even in the absence of any subband mixing effects. The effect on oscillator strength due to a quantum-well asymmetry was investigated theoretically for several exciton transitions. Figure 9 shows the theoretical values of f_{nm}/L_z depending on the asymmetry for the $C1$-$H1$, $C1$-$L1$, $C1$-$H3$, $C2$-$H2$, $C2$-$L1$, $C2$-$H3$, $C2$-$L2$, and $C3$-$H3$ excitons independently or with the combination of two transitions. The f_{nm}/L_z-versus-L_z relationships are presented for (i) a symmetrical well with $\Delta E_g(x = 0.25)$, (ii) an asymmetrical well with $\Delta E_g(x = 0.25)$ and $A(x' = 0.05)$, and (iii) an asymmetrical well with $\Delta E_g(x = 0.25)$ and $A(x' = 0.1)$. Variations of f_{nm}/L_z in the asymmetric cases can be compared to the symmetric-well case. Small variations are present for the $C1$-$H1$ and $C1$-$L1$ excitons whereas large changes exist for the $C3$-$H3$, $C2$-$L1 + C2$-$H2$, and $C2$-$H3 + C2$-$L2$ excitons. The large change of f_{nm}/L_z for the $C2$-$H3 + C2$-$L2$ and $C2$-$L1 + C2$-$H2$ excitons mainly comes from the variation of f_{nm}/L_z for the forbidden $C2$-$L1$ and $C2$-$H3$ excitons while the values for the allowed $C2$-$H2$ and $C2$-$L2$ excitons almost remain unchanged. A fit between the theoretical values of f_{nm}/L_z and the experimental data over a wide range of L_z, as shown in Fig. 10, is consistent with the assumption of insignificant asymmetry in the samples studied.

Figure 10 shows the calculated oscillator strength f_{nm}/L_z (Å^{-3}) and experimentally determined transition strength as a function of L_z for the same excitons as shown in Fig. 9 assuming symmetrical wells with $\Delta E_g(x = 0.25)$. Combined oscillator strength is used for the transitions of the $C2$-$H2$ and $C2$-$L1$ excitons and the transitions of the $C2$-$H3$ and $C2$-$L2$ excitons since some of those transitions are not readily resolvable. As is evident from the figure, the agreement between calculation and experiment is quite good. We also find that the oscil-

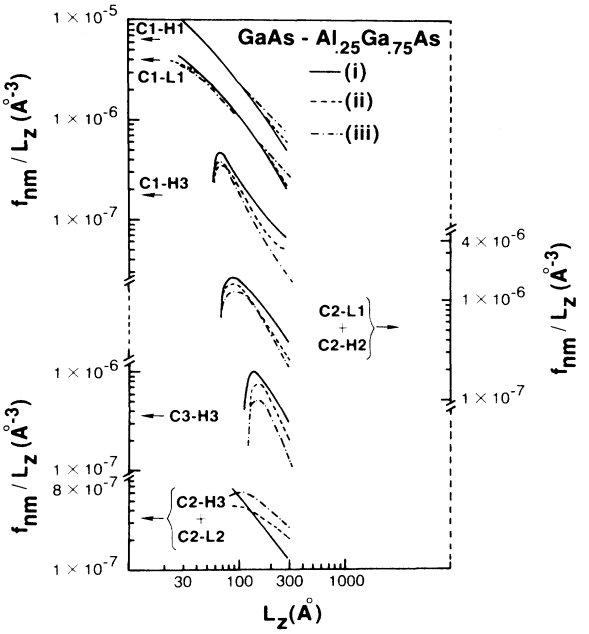

FIG. 9. Calculated values of $f_{nm}/L_z(\text{Å}^{-3})$ made with $m_h^*/m_0=0.34$ and $m_l^*/m_0=0.094$ for three types of the well: (i) symmetrical wells with $\Delta E_g(x=0.25)$, (ii) asymmetrical wells with $\Delta E_g(x=0.25)$ and $A(x'=0.05)$, and (iii) asymmetrical wells with $\Delta E_g(x=0.25)$ and $A(x'=0.1)$.

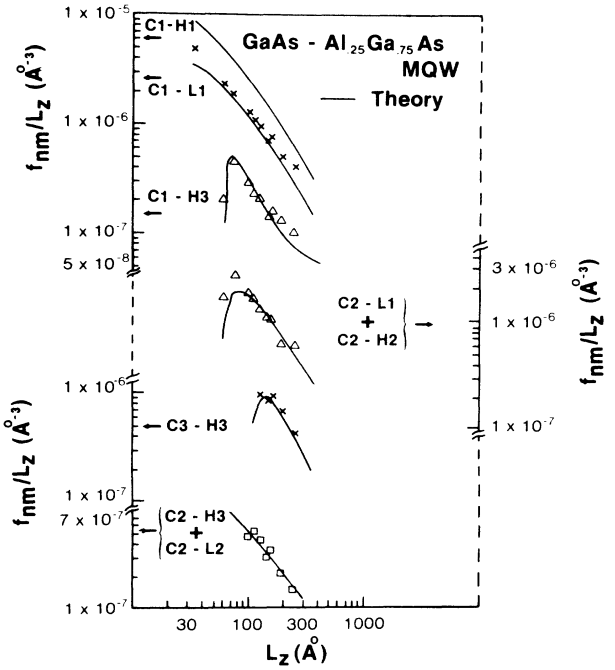

FIG. 10. The theoretical bulk oscillator strength f_{nm}/L_z as a function of well width for the $C1$-$H1$, $C1$-$L1$, $C2$-$L1$, $C2$-$H2$, $C1$-$H3$, $C2$-$H3$, $C2$-$L2$, and $C3$-$H3$ excitons. Experimentally obtained integrated area of photocurrent dips of the $C1$-$H1$ excitons was adjusted to the theoretical value of the $C1$-$H1$ oscillator strength. The theoretical values are obtained with $m_h^*/m_0=0.34$ and $m_l^*/m_0=0.094$ for symmetrical wells.

lator strength of $C2$-$H4$, $C4$-$H4$, and $C5$-$H5$ excitons, which are not shown in Fig. 10, agree well with calculated values with the symmetrical well of $\Delta E_g(x=0.25)$. The multiband effective-mass model with the valence-band mixing can thus explain the details of exciton transition energy and oscillator strength.

In conclusion, photovoltage-induced photocurrent measurements for $Al_xGa_{1-x}As$-GaAs multiple quantum-well structures grown by molecular-beam epitaxy have been performed. The relative minima (dips) of PC responses and the integrated areas of the dips are used to identify the exciton transition energies and to measure the oscillator strengths for several allowed and forbidden transitions, respectively. Forbidden transitions associated with $C1$-$H2$, $C1$-$H3$, $C2$-$H4$, $C3$-$L2$, and $C3$-$H5$ and superposition of the $C2$-$H2$ and $C2$-$L1$ excitons are clearly identified. Transition energies and oscillator strengths determined by PC measurements are well desribed by our theory. The sharing of oscillator strength between the $C2$-$H3$ and $C2$-$L2$ excitons is also observed for the first time. The above observations show that the multiband effective-mass model with the valence-band mixing can explain the details of exciton transitions rather well. The effects on exciton transition energy and oscillator strength due to a slight quantum-well asymmetry have been investigated. The asymmetry of the well was found to be insignificant for the present multiple quantum well structures.

ACKNOWLEDGMENTS

The work of P. W. Yu and G. D. Sanders was performed at the U.S. Air Force Avionics Laboratory under Contract Nos. F33615-84-C-1423 and F33601-82-C-1716 respectively. The work of the University of Illinois was supported by the U.S. Air Force Office of Scientific Research.

[1]R. C. Miller, D. A. Kleinman, W. A. Nordland, and A. C. Gossard, Phys. Rev. B **22**, 863 (1980).

[2]D. C. Reynolds, K. K. Bajaj, C. W. Litton, P. W. Yu, W. T. Masselink, R. Fischer, and H. Morkoc, Phys. Rev. B **29**, 7083 (1984).

[3]W. T. Masselink, P. J. Pearah, J. Klem, C. K. Peng, H. Morkoc, G. D. Sanders, and Y. C. Chang, Phys. Rev. B **32**, 8027 (1985).

[4]L. Shulteis and K. Ploog, Phys. Rev. B **30**, 1090 (1984).

[5]P. Parayanthal, H. Shen, F. M. Pollak, O. J. Glembocki, B. V. Shanabrook, and W. T. Beard, Appl. Phys. Lett. **48**, 1261 (1986).

[6]K. Yamanaka, T. Fukunaga, N. Tsukada, K. L. Kobayashi, and M. Ishii, Appl. Phys. Lett. **48**, 31 (1986).

[7]P. Blood, J. Appl. Phys. **58**, 2288 (1985).

[8]R. T. Collins, K. V. Klitzing, and K. Ploog, Phys. Rev. B **33**,

4378 (1986).
[9]H. J. Polland, Y. Horikoshi, R. Höger, E. D. Göbel, J. Kuhl, and K. Ploog, Physica **134B**, 412 (1985).
[10]P. W. Yu, D. C. Reynolds, K. K. Bajaj, C. W. Litton, J. Singh, C. K. Peng, T. Henderson, and H. Morkoc, Solid State Commun. **58**, 37 (1986).
[11]D. A. B. Miller, D. S. Chelma, T. D. Damen, A. C. Gossard, W. Wiegmann, T. H. Wood, and C. A. Barrus, Phys. Rev. B **32**, 1043 (1985).
[12]E. E. Mendez, G. Bastard, L. L. Chang, L. Esaki, H. Morkoc, and R. Fischer, Phys. Rev. B **26**, 7101 (1982).
[13]J. A. Kash, E. E. Mendez, and H. Morkoc, Appl. Phys. Lett. **46**, 173 (1985).
[14]G. D. Sanders and Y. C. Chang, Phys. Rev. B **32**, 5517 (1985); **31**, 6892 (1985).
[15]R. Dingle, in *Festkörperprobleme,* Vol. 15 of *Advances in Solid State Physics,* edited by H. J. Queisser, (Pergamon/Vieweg, Brauschweig, 1975), p. 21.
[16]H. J. Lee, L. Y. Juravel, J. C. Wooley, and A. J. Springthorpe, Phys. Rev. B **21**, 659 (1980).
[17]F. Bassani and G. P. Parravicini, *Electronic State and Optical Treatise in Solids* (Pergamon, Oxford, 1975), Chap. 5.
[18]R. C. Miller, D. A. Kleinman, and A. C. Gossard, Phys. Rev. B **29**, 7085 (1984).
[19]D. Bimberg, in *Festkörperprobleme,* Vol. 17 of *Advances in Solid State Physics,* edited by J. Treusch, (Pergamon, New York, 1977), p. 195.
[20]A. L. Mears and R. A. Stradling, J. Phys. C **4**, 122 (1971).
[21]R. C. Miller, A. C. Gossard, G. D. Sanders, Y. C. Chang, and J. N. Schulman, Phys. Rev. B **32**, 8452 (1985).